SIMULATION OF ROOT-MATTED SOIL CUTTING BY USE OF DISTINCT ELEMET METHOD

Bambang PURWANTANA[*)]

ABSTRACT

A numerical technique, the distinct element method (DEM), was used to simulate the mechanical behavior of root-matted soil. The conventional DEM was modified with introducing a tensile parameter on the mechanical relationship between the DEM elements. The validity of the modified model was investigated by conducting an experiment in which root-matted soil is cut by a blade. The simulation results indicate the appropriateness of the modified DEM. The effects of tension from the experimental results could be simulated by the DEM. This study has provided new and valuable information on the behavior of soil and root at cutting process.

Keywords: *Root-matted soil, modified DEM, tensile parameter, cutting*

1. INTRODUCTION

Distinct Element Method (DEM) is one of numerical technique that has potential for studying the behavior of discrete or granular material. The DEM is introduced originally by Cundall (1979) to analyze a collection of granular particles. The method has since been used to study many other type of discrete material, and also in some cases the continuum materials (e.g., Iwashita and Oda, 1998; Shimizu and Cundall, 2001). In the conventional DEM, the object is assumed as an assembly of discrete elements and the mechanical relationships between elements are determined by normal spring constant, tangential spring constant and frictional parameters. For specific purposes some modified DEM have been developed. Iwashita and Oda (1998) for example, introduce a rolling parameter on the elements. Momozu et al. (2003), introduce an adhesion parameter around the elements.

We have conducted a study on the cutting of root-matted soil. It was found that root-mat makes soil less cohesive in that soil pulverization was greater than that of simple soil. It was also found that the root-mat increased the cutting resistance, and the resistance force increased with root density and decreased with the moisture content (Purwantana et al., 2002). However we cannot see a real image of root-mat behavior inside the soil block under cutting. Therefore, further study on the behavior, especially micro-mechanical behavior, of the root-matted soil under cutting is proposed as it is essential to aid at furthering design of cutting device.

In this study, the DEM is applied to simulate the behavior of root-matted soil under cutting. The conventional DEM is modified by introduces a tensile parameter on the mechanical relationship between the elements. Soil and root are stated by collection of elements with different properties. The first objective of this study is to investigate the applicability of the modified computation model with comparisons between simulated results and experimental ones. The second is to clarify the relationship between the parameters of DEM elements and the mechanical properties of tested root-matted soil. In this study a two dimensional DEM with simple root-mat structure is applied; a three dimensional DEM with real root-mat structure will be targeted in future studies.

2. PRINCIPLE OF DEM

2.1. Expression of root-matted soil by DEM elements

DEM is based on the law of physics. It is often used to analyze the behavior of granular materials. The movement of the particle is controlled by equation of motion. In this study, root and soil are represented as assembly of two-dimensional circular elements, with different properties, as shown in Figure 1. The behavior of soil and root is analyzed by tracing the motion of each element that can be derived from the mechanical interaction between the elements.

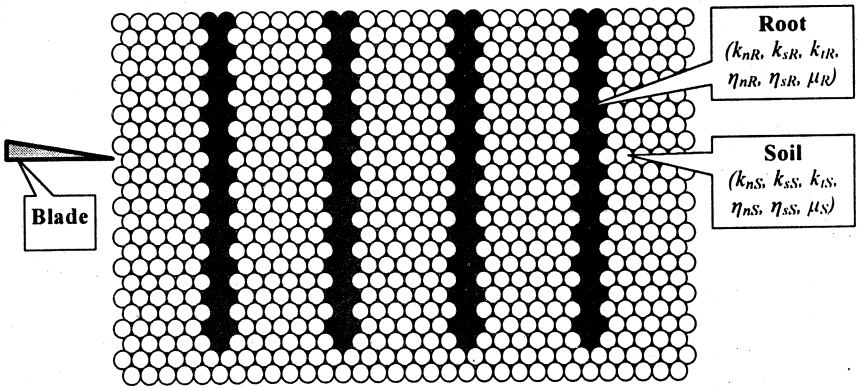

k	Spring	Suffix: n	Normal
η	Dashpot	s	Tangential
μ	Friction	t	Tensional
		R	Root
		S	Soil

Fig. 1. The root-matted soil model by circular elements

*) Departement of Agricultural Engineering, Faculty of Agricultural Technology, Gadjah Mada University, Bulaksumur, Yogyakarta 55281, Indonesia, E-mail: bambang_pur@lycos.com

Each element receives contact forces from contacting elements and/or sides of the blade. The magnitude of the contact force is determined by the relative displacement and relative velocity of the element. In the conventional DEM, it is assumed that an overlap is allowed between contacting ones, and the contact forces are calculated during the overlapping. In this study, a tensile force will be considered and therefore, the contact force will also be calculated when the elements depart from each other.

2.2. Conventional DEM

In order to derive the equation of motion, it is necessary to estimate the forces acting among elements. In the DEM simulation, the acting forces by an element to another are modeled by the vibration system as shown in Figure 2. A spring with a constant k, a dashpot with a coefficient of viscous damping η and a slider with a coefficient of friction μ are supposed to be between elements i and j. In the conventional DEM, in the normal direction, a no-tension joint is inserted to imply that there is no tension force when two elements depart from each other.

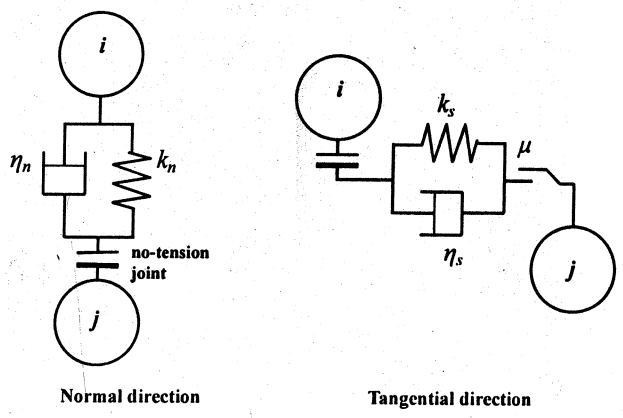

Fig.2. Mechanical relationships between elements of the conventional DEM

Figure 3 shows the schematic diagram of the contact between two elements. The normal direction n coincides with the line connecting between the centers of two elements while the tangential direction s perpendicular to the normal direction at the point of contacting elements. If the angle between the line connecting the centers of two elements and the X-axis is termed as α_{ij}, then

$$\cos\alpha_{ij} = \frac{(x_j - x_i)}{r_{ij}} \quad \text{and} \quad \sin\alpha_{ij} = \frac{(y_j - y_i)}{r_{ij}} \quad \text{where,}$$

$$r_{ij} = \sqrt{(x_j - x_i)^2 + (y_j - y_i)^2}$$

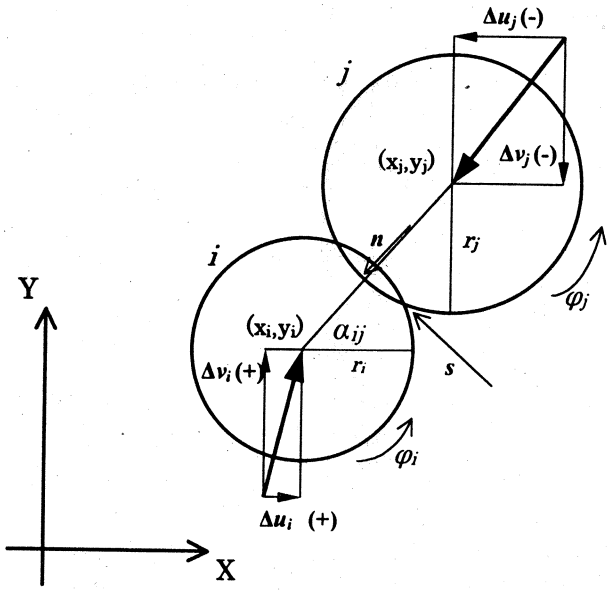

Fig. 3. Schematic diagram of element contact

The relative displacement of the element i to the element j in the normal direction Δu_n is expressed by Equation (1), and in the tangential direction Δu_s by Equation (2).

$$\Delta u_n = (\Delta u_i - \Delta u_j)\cos\alpha_{ij} + (\Delta v_i - \Delta v_j)\sin\alpha_{ij} \quad (1)$$

$$\Delta u_s = -(\Delta u_i - \Delta u_j)\sin\alpha_{ij} + (\Delta v_i - \Delta v_j)\cos\alpha_{ij} + r_i\Delta\varphi_i + r_j\Delta\varphi_j \quad (2)$$

Here Δu and Δv are the increment of displacement in x and y direction, $\Delta\varphi$ is the increment of rotation, and r is radius of the element. The suffix, n and s indicate normal and tangential directions; i and j indicate each element.

In the normal direction, the force due to the spring Δe_n and the force due to the viscous dashpot d_n are expressed by the following equations.

$$\Delta e_n = k_n \Delta u_n \qquad , d_n = \eta_n \frac{\Delta u_n}{\Delta t}$$

where Δt is the time interval of calculation. The increment of the force in the tangential direction due to the spring Δe_s and the force due to the viscous dashpot d_s are expressed by the following equations.

$$\Delta e_s = k_s \Delta u_s \qquad , d_s = \eta_s \frac{\Delta u_s}{\Delta t}$$

The spring force at time t, $[e_n]_t$, is obtained by adding the increment of the spring force e_n to the spring force at the previous step $[e_n]_{t-\Delta t}$ as follows:

$$[e_n]_t = [e_n]_{t-\Delta t} + k_n \Delta u_n \quad (3)$$

The normal contact force on the element i given by the element j is obtained by adding the force by the dashpot $[d_n]_t$ to the force by the spring $[e_n]_t$ as follows:

$$[f_n]_t = [e_n]_t + [d_n]_t = ([e_n]_{t-\Delta t} + k_n \Delta u_n) + \frac{\eta_n \Delta u_n}{\Delta t} \quad (4)$$

In the same way, the contact force in the tangential direction is calculated as:

$$[f_s]_t = [e_s]_t + [d_s]_t = ([e_s]_{t-\Delta t} + k_s \Delta u_s) + \frac{\eta_s \Delta u_s}{\Delta t} \quad (5)$$

The resultant forces which act on the element i in the horizontal, vertical and rotational directions, Fx, Fy and M, are obtained as follows:

$$[Fx_i]_t = \sum_j \left(-[f_n]_t \cos\alpha_{ij} + [f_s]_t \sin\alpha_{ij}\right) \quad (6)$$

$$[Fy_i]_t = \sum_j \left(-[f_n]_t \sin\alpha_{ij} - [f_s]_t \cos\alpha_{ij}\right) \quad (7)$$

$$[M_i]_t = -r_i \sum_j ([f_s]_t) \quad (8)$$

The acceleration of the element in the horizontal, vertical and rotational directions are given by

$$[\ddot{u}_i]_t = \frac{[Fx_i]_t}{m_i}, \quad [\ddot{v}_i]_t = \frac{[Fy_i]_t}{m_i}, \quad [\ddot{\varphi}_i]_t = \frac{[M_i]_t}{I_i} \quad (9)$$

In the calculation, the above equations are integrated to obtain the displacement in Δt. Then the same calculation is repeated by using the obtained displacement as an initial value for the next step of calculation.

2.3. Modified DEM

It is almost unable to simulate the block of root-matted soil if the root and the soil elements have complete discreteness. Therefore, a force that makes the elements pull each other should be considered. For this purpose, in this present modified DEM, a tensile spring k_t and a tensile dashpot η_t are installed between the elements as shown in Figure 4. When compression occurs, the conventional DEM is applied; when the elements begin to depart from each other, the modified model is applied. The tensile force work during the distance 'D' which can be settled as:

$$r_i + r_j < D \le (1 + c_d) \times (r_i + r_j) \quad (10)$$

where $c_d = f(r_i, r_j)$=coefficient of distance, and

$$D = \sqrt{(x_j - x_i)^2 + (y_j - y_i)^2}$$

Regarding the tensile characteristics obtained in the preliminary trial, the tensile force performance during separation follows the Maxwell model of combination of spring and dashpot. The tensile force is taken up initially by the spring. On displacement of the spring the dashpot element starts to move as well with an increasing rate, and takes up a correspondingly increasing force. When the spring reaches its maximum elongation, the whole force is taken up by the dashpot, moving at constant rate: the deformation rate versus time curve becomes horizontal. If the rate of elongation ε is assumed constant, the tensile force $[f_t]$ may be obtained by

$$[f_t] = e^{-\int \frac{k_t}{\eta_t} dt} \left\{ \int \varepsilon k_t e^{\int \frac{k_t}{\eta_t} dt} dt + C \right\} \quad (11)$$

where $\varepsilon = \dfrac{D - (r_i + r_j)}{(r_i + r_j)}$, and C is a constant. When the tensile-ability of the spring and dashpot reach its ultimate yield, the connection will cut.

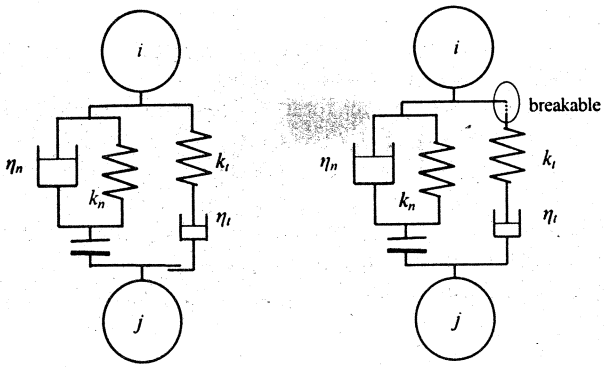

Fig. 4. Modified DEM by introducing tensional parameter k_t and η_t between the elements

3. EXPERIMENTS AND SIMULATION

3.1. Experimental procedure

The experimental apparatus consists of two guide rails (a slide and a screw guides), a force transducer, a blade and block of root-matted soil as shown in Figure 5. This was developed to confirm the root-matted soil model by the DEM. The blade travels horizontally when the screw guide is rotated.

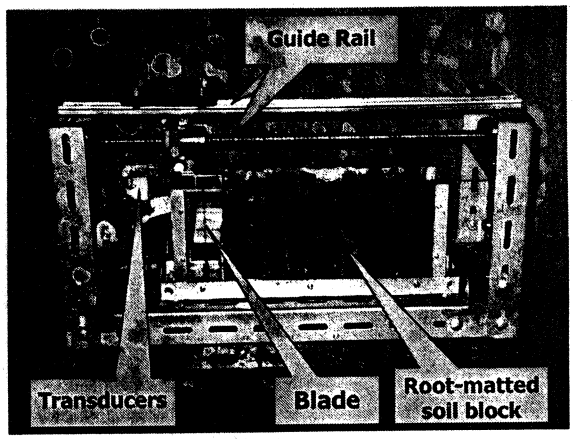

Fig. 5. The apparatus of the experiment

The experiments were carried out under the soil moisture content of 24.7% with soil cone index of 84 kPa. The details of the parameter setting are given in Table 1. The cuts were recorded with a high-speed video camera. The camera has a frame rate of 500s^{-1} at full frame mode. The images were saved to a personal computer. Three light bulbs (300 W each) were set up surrounding the apparatus in order to obtain clear images.

Table 1. Parameter setting of the experiment

Blade	-	width (mm)	25
	-	thick (mm)	5
	-	tip angle (°)	11.3
Soil	-	type	Sandy loam
	-	moisture content (%)	24.7
	-	Cone Index (kPa)	84
Root	-	diameter (mm)	4
	-	distance (mm)	10, 20
Cutting speed (m/s)			0.4, 0.8

3.2. Simulation procedure

In the simulation, the sizes of the root-matted soil block, blade, cutting depth, cutting speed and other parameters of cutting conditions were set up the same as in the experiment (Table 2). Table 3 shows the parameters used throughout the simulation. The radius of the elements was set to be 1.0 mm and the total number of the elements was counted as 2856. After DEM elements were placed in the container, the assembly was consolidated with gravity (compaction process) for 1.0 s. According to the parameters used in this simulation, the time interval Δt was set to be 1.0 x 10^{-5} s. The outputs of calculation were obtained every 1.0 x 10^{-2} s.

Table 2. Cutting conditions at simulation

Parameter	Value
Cutting speed (m/s)	0.4, 0.8
Cutting depth (mm)	35
Root diameter (mm)	4.0
Root distance (mm)	8, 12,
Size of root-matted soil block (l x h, mm)	20 120 x
Width of blade tine (mm)	80
Thick of blade tine (mm)	25
	5

Table 3. Parameters used in the simulation

Parameter	Soil	Root	Wa ll
Normal spring	1200	1300	120
constant (N/m)	800	12500	00
Normal tension	300	350	125
constant (N/m)	1.30	1.35	00
Tangential spring	0.65	0.70	300
constant (N/m)	0.75	0.75	0
Normal dashpot			4.10
constant (N.s/m)			2.05
Tangential dashpot			0.75
constant (N.s/m)			
Friction coefficient			

4. RESULTS AND DISCUSSIONS

4.1. Result of the experiment

The root-matted soil behaviors at several points in cutting stage, as an example, are shown in Figure 6. It can be seen that the soil and root near the blade moved forward following the movement of the blade. Soil loosening developed especially at the parts around the roots. Soil pulverization occurred near the blade. Purwantana *et al.* (2002) revealed that root-mat increased the resistance force of the soil and the force increased with root density. These results will be confirmed in the simulation.

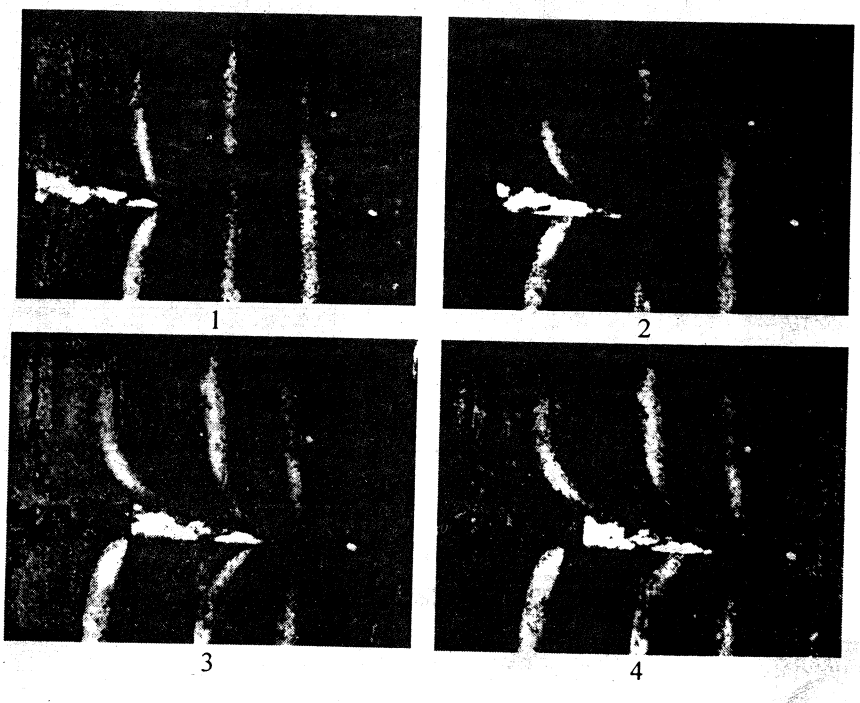

Fig. 6. The rot-matted soil behavior in the experiment

4.2. Result of the simulation

In the conventional computation of DEM, the elements have complete discreteness. There is no tension between DEM elements. However, if the tensile force between the elements is not considered, it would be impossible to simulate that the root-matted soil block could keep its shape under gravity as shown in Figure 7. The elements flow before cutting. Therefore, the modified model is used.

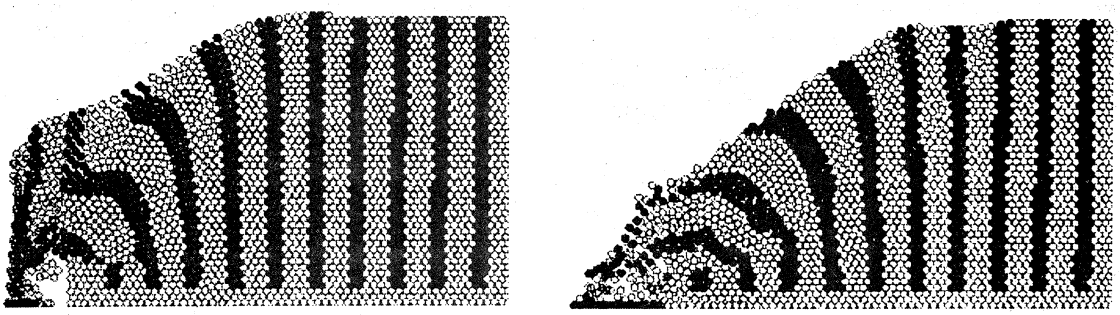

Fig. 7. Elements flow before cutting

In the application of the modified DEM, in this simulation, the effect of coefficient of distance *cd* was examined. Figure 8 shows some results of the examinations. The effect of the coefficient of distance appeared in the behavior of elements. At the *cd* of 0.04 to 0.08, some elements still easily apart from the block. With the increase of *cd*, the block becomes rigid and the detached elements were formed as clods. Comparing these results with those of the experiment, the simulation with the coefficient of distance between 0.12 and 0.16 can best simulate the behavior of the root-matted soil in the experiment. We employed *cd* of 0.125 throughout the simulation.

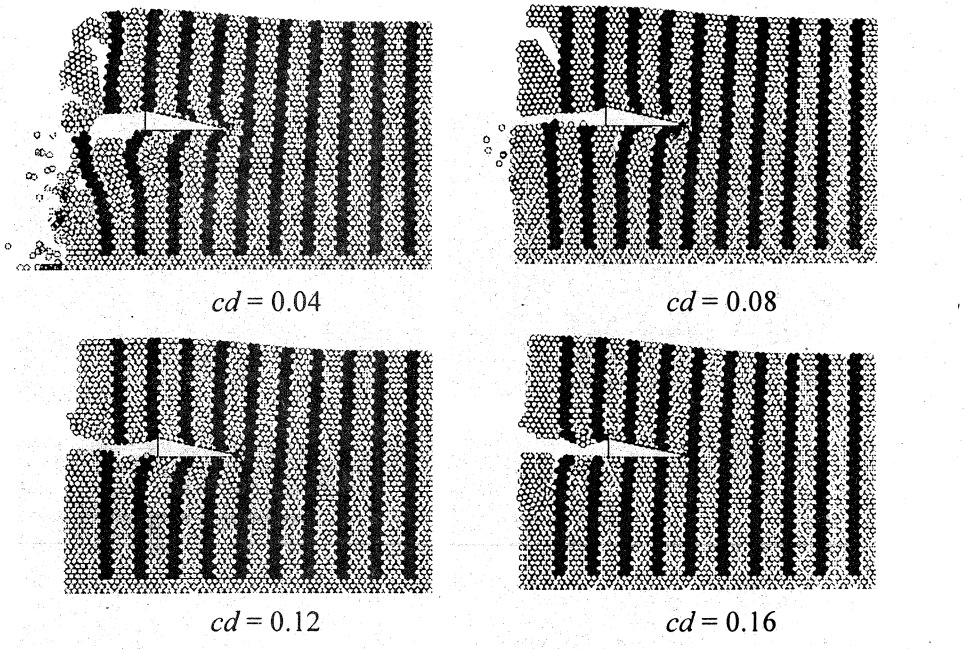

Fig. 8. The effect of coefficient of distance *cd* on the behavior of elements

Some results of the simulations, at cutting speed of 0.4 m/s and root distance of 12 mm, are as examples shown in Figure 9. The soil elements are brushed in light color and the root elements are in dark color. The loosening and pulverization developed at the soil elements part especially at the vicinity near the blade and around the root. The clod departed and moved slightly forward following the movement of the blade. With the introduction of tensional parameter, the elements were not dispersed in individual discrete elements. The elements near the blade moved forward in a greater displacement than the elements that far from the blade. Although the result was not perfectly same as in the experiment, it can be said that the tendency of the behavior was similar to that of root-matted soil in the experiment.

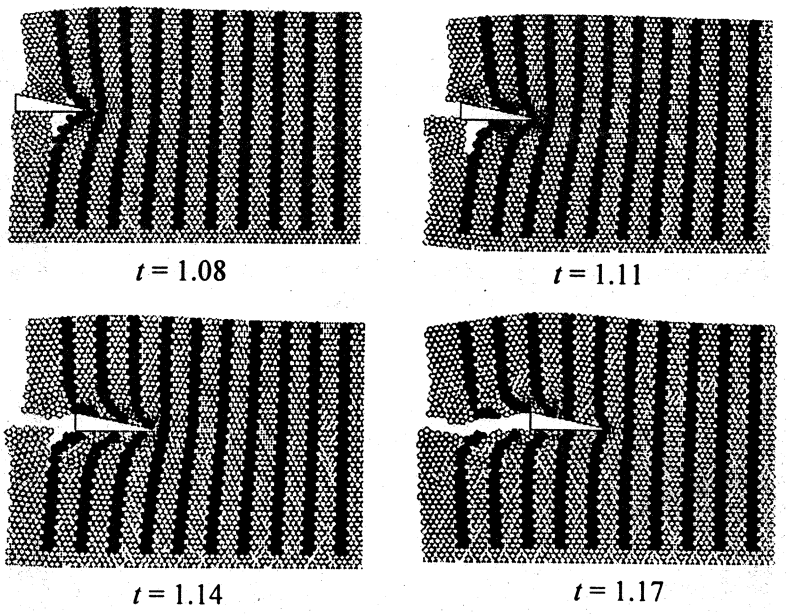

Fig.9. Results of simulation at several points of cutting stage

Figure 10 shows an example of the distribution of force works on the soils and roots elements. The light color was low force and the darker the higher. It can be seen that in general the root elements received greater force than that of the soil elements. It is agree with our previous experimental result that roots performed greater resistance to cutting than the soil (Purwantana *et al.* 2002).

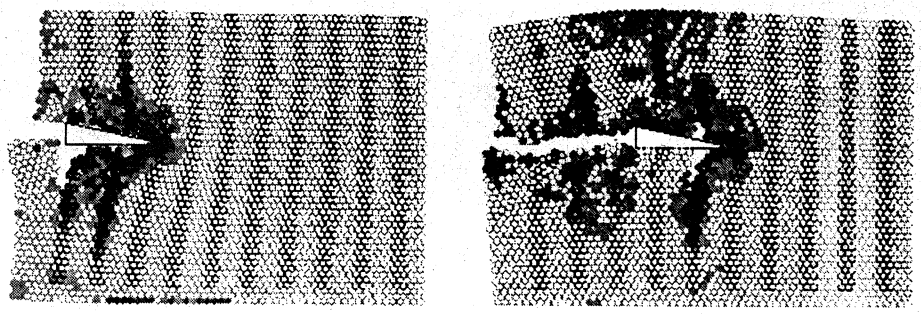

Fig. 10. Force distributions on the elements

The cutting resistance of the experiment and simulation are shown in Figure 11. The tendency is shown, but there is difference in magnitude. The resistance force in the simulation is apparently smaller than that of the experiment. It could be that although a tensional parameter is considered, the elements, which are circular, are still unstable. The acquired data of elements rotation shows that elements contacting with the blade were rotated by the penetration of the blade surface. In further study, this problem should be discussed such as by introducing a sufficient parameter that may resists the rotating of the elements.

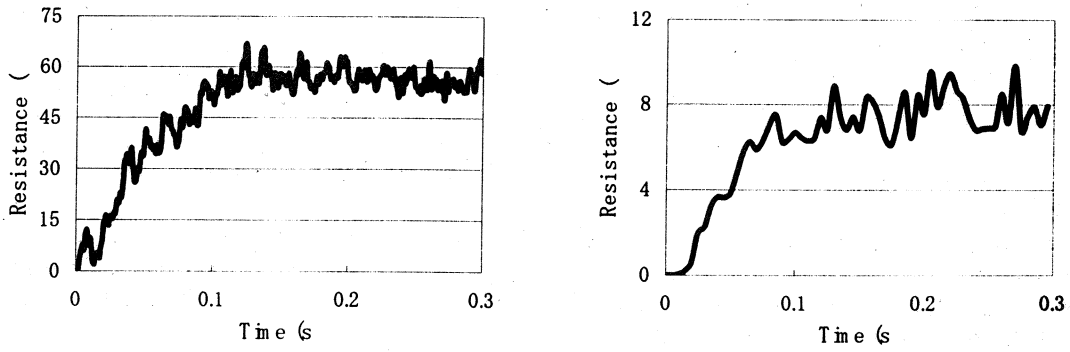

(a) experiment (b) simulation

Fig. 11. The cutting resistance of the experiment and the simulation

Figure 12 shows a comparison of element movement and force distribution of the cutting of simple and root-matted soils. It is clear that the root increased the resistance forces on the blade. The root also increased soil loosening of the block. This result was similar to that of the experimental ones. Therefore, it can be said here that the proportion of the value of spring and tensile constants between the soil and the root elements are appropriate enough.

In the simulations, soil loosening phenomena and reaction force had some variations because of the changing of cutting speed and root density. Figure 13 shows the root-matted soil behavior and forces work on the particles when the cutting speed was varied. The light color was low force and the darker the higher. A slightly greater soil loosening developed when the cutting speed was increased. The force work on the elements was also slightly greater at the higher speed.

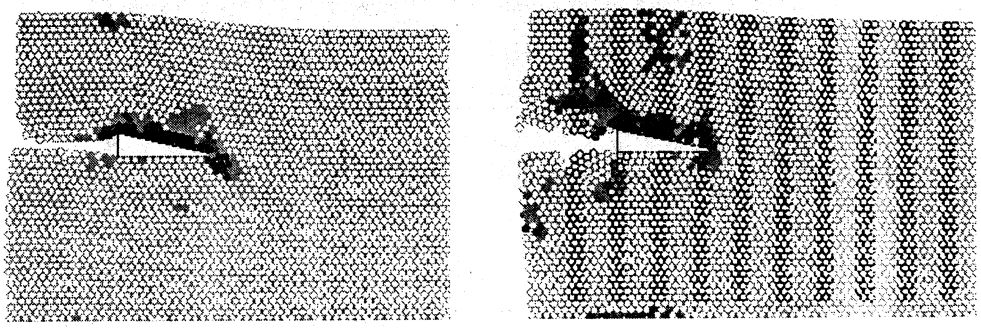

(a) simple soil (b) root-matted soil

Fig. 12. Comparison of element movement and force distribution on the simple and root-matted soils

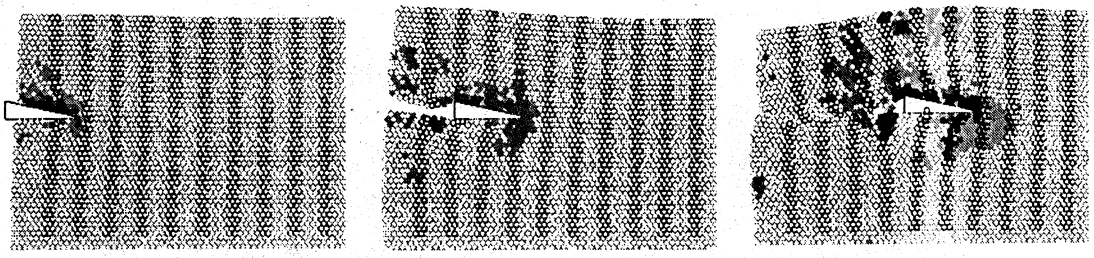

(a) $v = 0.4$ m/s

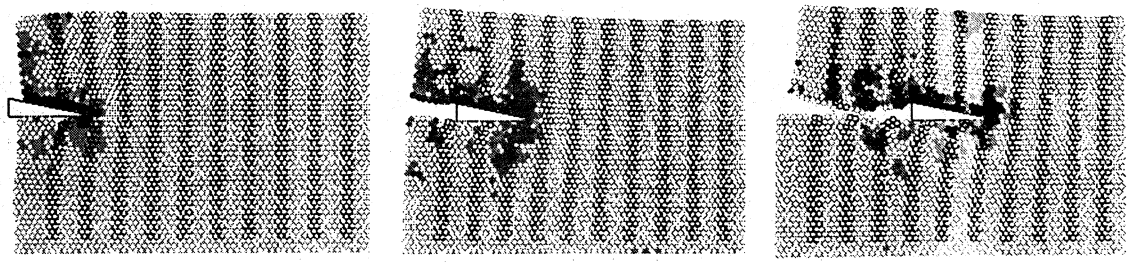

(b) $v = 0.8$ m/s

Fig. 13. Element and resistance force behavior at two different cutting speeds; v: cutting speed

The results of simulated cutting process at different root densities are shown in Figure 14. The soil loosening was observed slightly larger at the root-matted soil with greater density. The increase in root density resulted greater force work on the elements. These results give useful information for the theoretical consideration on the resistive force acting on blade in the root-matted cutting task.

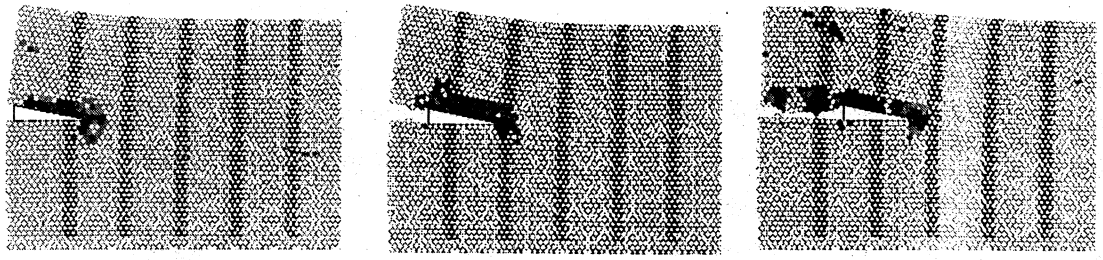

(a) $d = 20$ mm

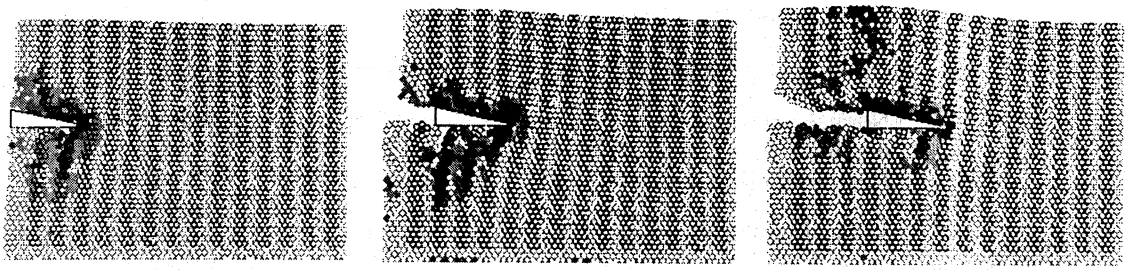

(a) $d = 8$ mm

Fig. 14. Element and resistance force behavior at two different root densities; *d*: root distance

In general, the simulation results indicate the validity of the modified DEM. The dynamics behavior of root-matted soil could be represented in the simulation. Despite the fact that some improvements are required, the study confirmed that the modified contact model could expand the applicability of DEM to the dynamic behavior of root-matted soil.

5. CONCLUSIONS

The modified DEM was applied to simulate the behavior of root-matted soil. The conventional DEM was modified by introduces a tensile parameter that work up to certain distance when the DEM elements departed each other. An experiment and simulation of root-matted soil cutting were conducted to investigate the validity of the modified model. Some characteristics phenomena of the experiment, i.e. soil loosening, root deflection, clod movement and cutting resistance, are reproduced in the simulation. The effects of cutting speed and root density obtained from the experiment results can also be simulated by the modified DEM.

Acknowledgements

I wish to express my warmest gratitude to Dr. Masatoshi Momozu (Kyoto University) for his assistance in developing the DEM program used in this study.

REFERENCES

Cundall, P.A., and Strack, O.D.L. 1979. A discrete numerical method for granular assemblies. Geotechnique, 29(1):47-65

Iwashita, K., and Oda, M. 1998. Rolling resistance at contacts in simulation of shear band development by DEM. Journal of Engineering Mechanics, 124(3):286-292

Momozu, M., Oida, A., Yamazaki, M., and Koolen, A.J. 2003. Simulation of a soil loosening process by means of the modified distinct element method. Journal of Terramechanics, 39(3):207-220

Purwantana, B., Horio, H., Kawamura, T., Shoji, K. 2002. A Flail-Type Rotary Cultivator for Introducing Swampland in Indonesia; Cutting Characteristics of Grass, Root-Mat and Topsoil. Proceeding of the International Agricultural Engineering Conference, Wuxi, China, November 28-30, 2002: 430-436.

Shimizu Y, Cundall P.A. 2001. Three dimensional DEM simulations of bulk handling by screw conveyors. Journal of Engineering Mechanics, 127(9):864-872

Nomenclature

k_n, k_s	Normal and tangential spring constants between elements
η_n, η_s	Normal and tangential coefficient of viscous damping between elements
μ	Coefficients of friction between elements
α_{ij}	Angle between elements *i* and *j* toward *X* axis
x_i, x_j	*X* coordinate of the element *i* and *j*
y_i, y_j	*Y* coordinate of the element *i* and *j*
r_{ij}	Distance between the centers of the elements *i* and *j*
$\Delta u_n, \Delta u_s$	Normal and tangential relative displacements of the elements *i* to the element *j* during Δt
$\Delta u_i, \Delta u_j$	Horizontal displacements of the elements *i* and *j* during Δt
$\Delta v_i, \Delta v_j$	Vertical displacements of the elements *i* and *j* during Δt
r_i, r_j	Radius of elements *i* and *j*
$\Delta\varphi_i, \Delta\varphi_j$	Rotational displacements of the elements *i* and *j* during Δt
$\Delta e_n, \Delta e_s$	The force due to spring in normal and tangential directions
d_n, d_s	The force due to viscous dashpot in normal and tangential directions
Δt	Time interval
$[e_n]_t, [e_n]_{t-\Delta t}$	Normal spring forces on an element at time *t* and *t*-Δt
$[e_s]_t, [e_s]_{t-\Delta t}$	Tangential spring forces on an element at time *t* and *t*-Δt
$[d_n]_t, [d_s]_t$	Normal and tangential damping forces on an element at time *t*
$[f_n]_t, [f_s]_t$	Normal and tangential contact forces on an element at time *t*
$[Fx_i]_t$	Horizontal resultant force on the element *i* at time *t*
$[Fy_i]_t$	Vertical resultant force on the element *i* at time *t*
$[M_i]_t$	Resultant moment on the element *i* at time *t*
I_i	Moment of inertia on the element *i*
$[\ddot{u}_i]_t, [\ddot{v}_i]_t, [\ddot{\varphi}_i]_t$	Acceleration of the element *i* in the horizontal, vertical and rotational directions
D	Distance of the elements *i* and *j* during departs
c_d	Coefficient of distance
$[f_t]$	Tensional forces